Journal of Engineering and Sustainable Development
https://jeasd.uomustansiriyah.edu.iq/index.php/jeasd
https://doi.org/10.31272/jeasd.28.2.9

Vol. 28, No. 02, March 2024
ISSN 2520-0917

Original Research

PERFORMANCE OF SCREW HORIZONTAL AND BRIDGE LINKAGE PHOTOVOLTAIC ARRAY CONFIGURATIONS

Mohammed Osamah Subhi*[1], Wafaa Saeed Majeed[2]

[1,2]*Electrical Engineering Department, College of Engineering, Mustansiriyah University, Baghdad, Iraq*

Received 03/12/2022 ***Revised 23/10/2023*** ***Accepted 05/02/2024***

Abstract: Due to partial shading effects on the productivity of solar panels which in turn negatively impacts the performance characteristics of photovoltaic systems, researchers work on different studies to overcome this phenomenon and improve solar system productivity. Therefore, this study aims to investigate different techniques to enhance the output power, fill factor, and efficiency of the PV system by reducing the number of local maximum power peaks, power losses, and mismatch losses. The configurations include a novel static reconfiguration technique, called a Screw Horizontal photovoltaic array, and a recently developed technique known as a Bridge Linkage array. Both of these are modeled using MATLAB/Simulink software and examined during six shading patterns. The novelty of this study is that we combined the above static reconfiguration technique with another modern technique called blocking and bypass diode technology to prevent the effect of reverse current and hotspot phenomena respectively. According to the results, the Bridge Linkage configuration performs the most efficiently under partial shading conditions compared to the Screw horizontal PV array configuration.

Keywords: *Bypass diodes; blocking diodes; partial shading condition; photovoltaic system; sustainable energy*

1. Introduction

Environmental pollution is widespread as a result of population growth, rising electricity demand, and the global consumption of millions of tons of fossil fuels each year. This hurts organisms generally and humanity especially. As a result, oil, gas, and petrochemical prices fluctuate, despite coal being the world's main energy source[1]. Various sustainable energy sources, especially in electric power generation, can be used instead of fossil fuels. Sustainable energy sources include wind, nuclear, geothermal, hydraulic, solar, and biofuels. Biofuels are a biodegradable fuel source derived from wood, agricultural, and animal waste [2]. However, electricity can be produced in vast amounts by using solar and wind energies [3-6]. The study also found that green energy consumption decreases CO2 emissions, while nonrenewable energy consumption and economic growth increase CO2 emissions [7]. PV technology is suitable for producing electricity in different countries because of the uniform distribution of solar radiation in the world. Some countries are located in or near the solar belt and have long sunny hours per day, which makes them in an optimum location to take advantage of solar technologies [8]. In recent years, solar power has been considered an excellent alternative due to its availability, carbon-free, and sustainability without any contamination such as conventional fossil fuels [9]. However, installation costs have

*Corresponding Author: mohammed.osamah@uomustansiriyah.edu.iq

decreased gradually and its capacity has grown dramatically simultaneously [10-12].

Solar energy can be converted into electricity via two methods: concentrated solar power (CSP) and photovoltaic (PV) [13]. By concentrating the sun's rays, concentrated solar power (CSP) generates heat and steam that rotate conventional turbines [14]. Photovoltaic cells (PVs) were invented in 1954 by Bell Laboratory in the United States [15]. PV technology can be employed for standalone systems for rural telephone stations, transmitting stations, emergency telephones for high-speed roads, and cathodic protection. Also, it can be used for operating water pumps that are used for drinking purposes, as well as irrigation, and for street lights, parks, residential buildings, heating, and cooking [16]. Variations in solar irradiation and temperature may age PV modules and reduce power production due to higher mismatch losses in the photovoltaic module [17-18]. On the other hand, high temperatures may cause PV modules to delaminate, create bubbles, and cause corrosion [19]. However, the construction of large solar farms will reduce the consumption of oil and gas particularly. In summary, partial shading phenomena cannot be predicted and have been viewed as the most common problem that leads to the reduction of energy productivity produces hotspots on the PV module's surface, which causes the system's temperature to increase, and the shaded modules consume the power of the non-shaded modules and dissipate heat [20-21].

In this study, we combine between two techniques that can enhance the output of PV arrays during shading conditions. Firstly, both blocking and bypass diodes are used, the blocking diode is connected in series with each PV string, and the bypass diode is connected in parallel with each PV module[22]. Although the blocking diode has a small voltage drop (about 0.7V, 0.4V, and 0.025V for silicon, Schottky, and smart diodes, respectively [23]) and the shaded PV module will be isolated from producing current by bypass diode [24], but blocking diode provides high protection against reverse current by ensuring the current flows from PV modules of each string to the terminal output and blocks reverse current from the discharging battery to the solar panels when solar irradiance is absent [25]. Bypass diode provides high protection against hotspot phenomena that can burn solar farms during shading conditions [26], [27]. Secondly, the Screw Horizontal (S-H) and Bridge Linkage (B-L) static reconfiguration techniques of PV arrays are compared under five shading levels. A PV array's non-linear power-voltage characteristic curve has only one peak when all modules of the array receive the same amount of light; otherwise, when partial shading occurs, the P-V characteristic curve has more than one peak point. Among these peaks, only one represents true maximum power, and the others are called local maximum power peaks (LMPP) [28]. However, the procedure of this study is shown as a flowchart in Fig. 1.

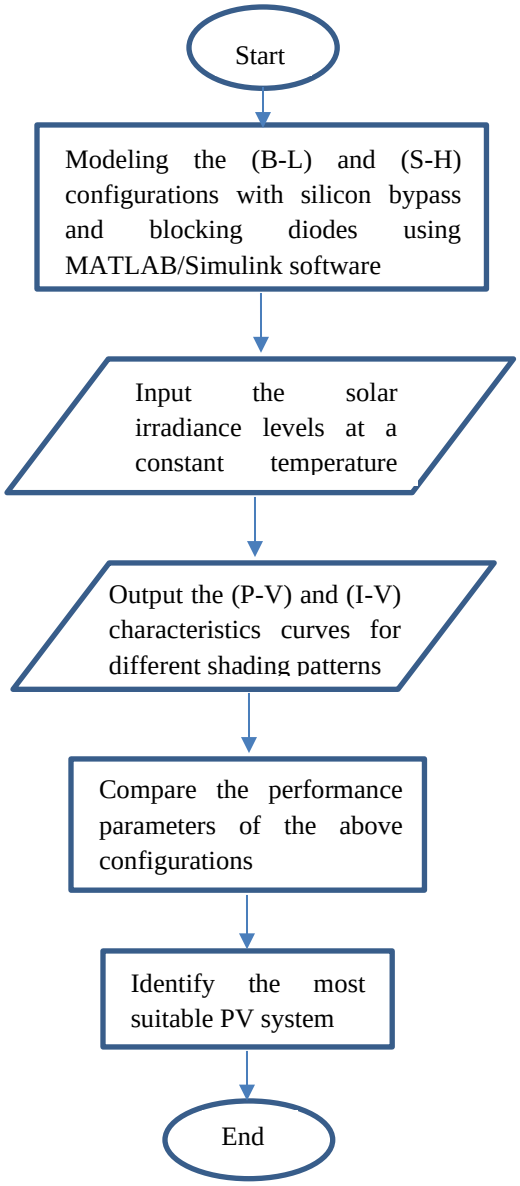

Figure 1. Flowchart of the proposed study

2. Related Works

Several topologies of photovoltaic array configurations have recently been investigated. The analysis results in [29] show the effect of shading on the number of maximum power points, however, in [30] the performance of asymmetrical PV array configurations was examined using 6x5 and 5x6 size arrays. As a result, the total cross-tied (TCT) of the 5x6 array produces the highest output power during all shading levels as compared to conventional PV array configurations. Additionally, the current injection method has been proposed in various kinds of array topologies. By adding a current source in each row of the 4x4 TCT array configuration, the authors in [31] proposed a novel PV array configuration to enhance the performance of the PV system. However, this method is quite expensive compared to the other methods, and it requires frequent maintenance to avoid system damage. It works by injecting current into each row of the PV array when affected by PSCs. This increases the current generated on the PV array to ensure that all PV rows operate with an even current. The authors in [32] proposed an intelligent reconfiguration technique that required a large number of switches and sensors. This method is done by dividing the PV modules in the array into a fixed end and an adaptive bank. Furthermore, when the PV modules in the fixed end are shaded or malfunctioned, they are switched into the adaptive bank. Theoretically, the TCT configuration is the most effective configuration for improving the global maximum power peak (GMPP) under a shading condition since all modules are cross-tied and series connections are eliminated. Due to the high number of cross-ties in this setup, cable losses are significantly higher in practice [33]. An algorithm based on dynamic reconfiguration is discussed in [34], in which the PV array is split into two parts - male and female. By using current sensing units to measure the current produced by each row of male and female parts, the controller couples a row of male parts generating the maximum current with a row of female parts generating the minimum current, resulting in even current generation in all PV rows. A similar kind of dynamic reconfiguration algorithm is proposed

in [35], where the switching operation is done in two steps to achieve the high-power enhancement. In the first step, the PV array is allowed to operate at its optimal array size, and then the system is switched to the second step when it is affected by uneven irradiance or other faults. This method minimizes the number of controls and measuring units in comparison with the previous one. Therefore, the overall cost will be reduced and the period between the establishment of the reconfiguration pattern will be shortened. A new method for configuring PV arrays is discussed in [36] according to the static reconfiguration technique. This method compares Parallel-Series (P-S), Total Cross Tied (TCT), and Sudoku puzzle array configurations under six shading patterns. In all shading patterns, the simulation results show that its power output is superior to the other configurations. It also performs more efficiently with minimal mismatch losses, making it a very practical design for any size of PV system. Furthermore, it is easy to implement and does not require any additional devices, sensors, or controllers. The researchers in [37] discuss a firefly algorithm (FA) that involves switches to reconfigure the PV module position during non-uniform shading to solve the current problems of unequal dispersion of shading affecting solar panels, multiple peaks, and hotspot phenomena that reduce solar efficiency and lead to power losses. By using cross-link switches between parallel strings of PV arrays, the authors in [38] examined the performance of Parallel-Series (P-S), Bridge Linkage (B-L), and Honey combo (H-C) configurations array with the proposed Adaptive cross-tied (A-CT) configuration that uses 4X5 of 20W PV modules. Therefore, the simulation results demonstrate that the A-CT PV array configuration has low wiring losses because it has fewer cross-tied connections between the parallel strings than conventional TCT, which is particularly beneficial for large PV plants. A study [39] compares the Total Cross Tide (TCT), Parallel Series (P-S), and Sudoku Puzzle Patterns with novel PV array configurations called Screw Horizontal (S-H) and Screw Vertical (S-V) Patterns under six shading levels. However, the researchers found that both (S-H) and (S-V) PV arrays performed better in performance analysis than conventional configurations.

We observe from different studies that the researchers have found several techniques to enhance the performance of PV array systems during nonuniform irradiance conditions, these techniques are static reconfiguration, dynamic reconfiguration, and diodes techniques. Dynamic reconfiguration of the PV array is an optimum method for reducing mismatch power loss under partial shading [40]. This is done by distributing shading effects uniformly throughout the array to provide a uniform row current. This technique depends on the type and position of shading. Although this solution is expensive, it increases the amount of power generated [41]. Hence, the maximum power output of the shaded and unshaded modules can be utilized [42]. It’s worth noting, the other two techniques are taken into account in this study.

3. Performance Equations

The most common parameters that directly affect the performance of PV array systems are Mismatch Losses (ML)[25], Power Losses (PL)[43], Efficiency (ɳ)[39], Fill Factor (FF) [33], and Number of Local Maximum Power Peaks (LMPPs) as shown in Equations (1) to (5).

$$ML(W) = P_{m(STC)} - P_{m(PSC)} \quad (1)$$

$$PL\ (\%) = \frac{ML}{Pm(STC)} \times 100 \quad (2)$$

$$\eta\ (\%) = \frac{V_{mp} \times I_{mp(PSC)}}{V_{mp} \times I_{mp(STC)}} \times 100 \quad (3)$$

$$FF\ (\%) = \frac{V_{mp} \times I_{mp(PSC)}}{V_{o.c} \times I_{s.c\ (STC)}} \times 100 \quad (4)$$

$$LMPP's = \text{Sum of peaks in P} - \text{V curve characteristic} - 1 \quad (5)$$

Where STC, PSC, P_m, V_{mpp}, I_{mpp}, $V_{o.c}$, and $I_{s.c}$ denote Standard Test Condition ($\frac{1000W}{m^2}$ &25c°), Partial Shading Condition, Maximum Output Power, Voltage at Maximum Power, Current at Maximum Power, Open Circuit Voltage, and Short Circuit Current respectively. Despite this, there are multiple peaks along the P-V characteristic curve when partial shading is applied. The actual maximum power is represented by only one peak among these peaks. Global maximum power peaks (GMPPs) are defined as MPPs with the highest power and local maximum power peaks (LMPPs) are MPPs with lower power. In other words, excellent performance occurs when P-V characteristics are smooth and LMPPs are few.

4. Mathematical Modelling

PV systems need much more energy than one solar cell can produce. However, we must connect them in parallel and series to obtain the optimum voltage and current. Fig. 2 shows a typical circuit diagram of a single-diode photovoltaic cell, which features an anti-parallel diode, a photon current source, and a series and shunt resistance. We can get information about a PV cell variable using Thevenin, Norton [44], or other equivalent circuit analysis methods [10]. Nonlinear Equation (6) shows the output current of a single PV cell [45]. To solve this equation, we must use the mathematical iteration method.

$$I_{pv} = I_{ph} - I_o \left[\exp\left(\frac{q(V_{pv}+I_{pv}R_s)}{AN_sKT}\right) - 1\right] - \frac{V_{pv}+R_sI_{pv}}{R_p} \quad (6)$$

Where I_{pv}, I_{ph}, and I_o indicate to current of the PV cell, Photo-current, and reverse saturation diode current respectively. Also, q, V_{pv}, R_s, and A refer to the charge of the electron (1.6×10^{-19} C), the Output voltage of the solar cell, Series resistance, and the Ideal factor respectively. In addition to the above, N_s, K, T, and R_p indicate the number of series solar cells, Boltzmann constant (1.38×10^{-23} J/K), Temperature of the solar cell, and Parallel resistance respectively. Screw horizontal (S-H) configuration array is constructed using Equations (7) and (8), depending on the size of the array generally and the number of columns specifically, where these equations are applied to odd and even numbers of columns, respectively [39].

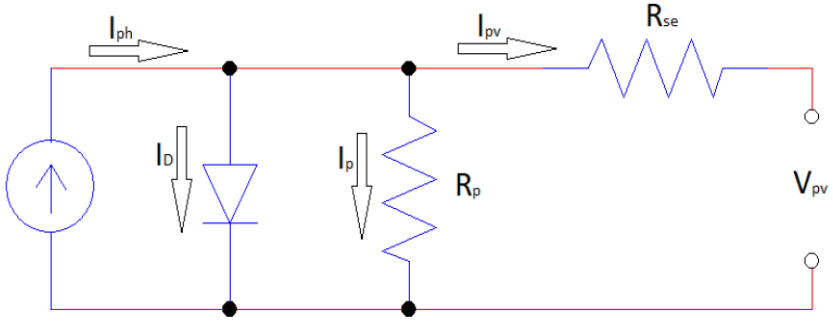

Figure 2. Equivalent circuit of singe diode photovoltaic cell.

$$PV_{ROW_k} = [P_{l\,m}] = [(1)(k)\ (2)(k+(z-1))\ (3)(z+1)\ (4)(k+(z-2))\ (5)(z+2)\ \dots \\ (z-1)\left(k+\left(\left(\frac{z+1}{2}\right)-1\right)\ (z)\left(k+\left(\frac{z+1}{2}\right)\right)\right] \quad (7)$$

$$PV_{ROW_k} = [P_{l\,m}] = [(1)(k)\ (2)(k+(z-1))\ (3)(k+1)\ (4)(k+(z-2))\ (5)(k+2)\ \dots \\ (z-1)\left(k+\left(\left(\frac{z+2}{2}\right)-1\right)\ (z)\left(k+\left(\frac{z+2}{2}\right)\right)\right] \quad (8)$$

This study compares Screw Horizontal (S-H) performance parameters with Bridge Linkage (B-L) photovoltaic 9x9 array configurations during different shading patterns. A bridge linkage (B-L) configuration is based on total cross-tied (TCT), but the main advantage over TCT is that it has fewer ties, installation time, and cable losses than TCT. To construct a 9x9 screw pattern array configuration, the mathematical Equation (7), substituting the values of (k) indicating the number of rows, and (z) representing the number of columns size, is used. As a result, first row includes P11, P29, P32, P48, P53, P67, P74, P86 and P95, second row includes P21, P39, P42, P58, P63, P77, P84, P96 and P15,third row includes P31, P49, P52, P68, P73, P87, P94, P16 and P25, fourth row includes P41, P59, P62, P78, P83, P97, P14, P26 and P35, fifth row includes P51, P69, P72, P88, P93, P17, P24, P36 and P45, sixth row includes P61, P79, P82, P98, P13, P27, P34, P46 and P55, seventh row includes P71, P89, P92, P18, P23, P37, P44, P56 and P65, eighth row includes P81, P99, P12, P28, P33, P47, P54, P66 and P75 and the last row includes P91, P19, P22, P38, P43, P57, P64, P76 and P85.

5. Results and Discussion

This study discusses two topology methods: The Diodes method and the Static reconfiguration method. Therefore, we compare two 9x9 arrangements, the first arrangement uses silicon bypass and blocking diodes along with a screw horizontal photovoltaic array, and the second arrangement uses similar diodes but with a bridge linkage static photovoltaic array. Thus, it is necessary to design and model different topologies with computer software such as Matlab/Simulink, Scilab, NI Multisim, or PSIM to evaluate the effects of shading on the behavior of I-V and P-V characteristics of photovoltaic systems. The simulation method is simpler and cheaper than the practical method, which allows a large number of PV modules to be connected or modified quickly and easily. Moreover, the transient response of the P-V and I-V characteristic curves of the system can be observed clearly in the simulation analysis, and a large number of complex nonlinear equations or iterations can also be solved more easily. Therefore, the study investigated possible solutions and used several tools of MATLAB/Simulink to explore shading's effects on PV modules. Thus, Fig. 3(d) shows three subsystem blocks that are modeled and implemented using MATLAB/Simulink. Two of these represent the suggested PV configurations and one represents the irradiance block. However, the content of the subsystem irradiance block is shown in Fig. 3(c). as well as, the proposed shading patterns are shown in Fig. 4. It is worth noting that the PV modules specifications at Standard Test Conditions

(STC) that we use to build proposed arrays are voltage at open circuit ($V_{o.c}$), current at short circuit ($I_{s.c}$), current at maximum power (I_{mp}), voltage at maximum power (V_{mp}) and rated power (P_{max}) which are 11.5V, 1.25A, 1.1A, 9.09V, and 10W respectively. Therefore, due to environmental variation especially temperature and solar radiation, the practical system will be different from (STC). During random shading, Figure 4a shows that the output power of the Screw Horizontal configuration is 352.11W and for the Bridge Linkage configuration is 394.2W. As shown in Fig. 4b, the Screw Horizontal and Bridge Linkage configurations generate an output power of 590.2W and 631.6W, respectively, under short and narrow shading conditions. However, when partial shading conditions are short and wide as shown in Fig. 4c, Screw Horizontal will generate 427.4W and Bridge Linkage will generate 434.5W. The Screw Horizontal and Bridge Linkage configurations, as shown in Fig. 4d, produce a maximum power of 554.8W and 620.1W during the partial shading test, whereas the long and wide partial shading test in Fig. 4e generates maximum power of 398.3W and 454.3W respectively. Fig.5 to 9 show the simulation results that show Power versus Voltage (P-V) and Current versus Voltage (I-V) characteristic curves during five levels of shading patterns: random, S&N, S&W, L&N, and L&W.

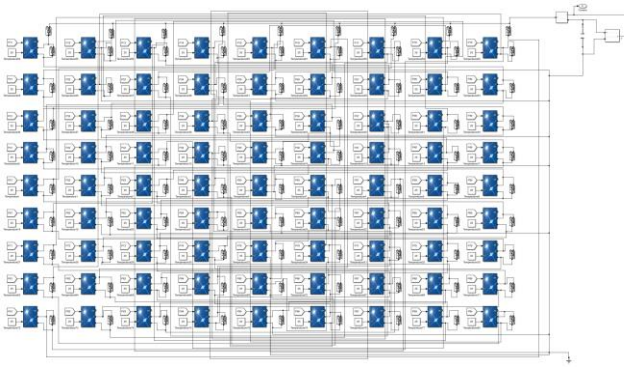

a) Screw Horizontal PV Array

b) Bridge Linkage PV Array

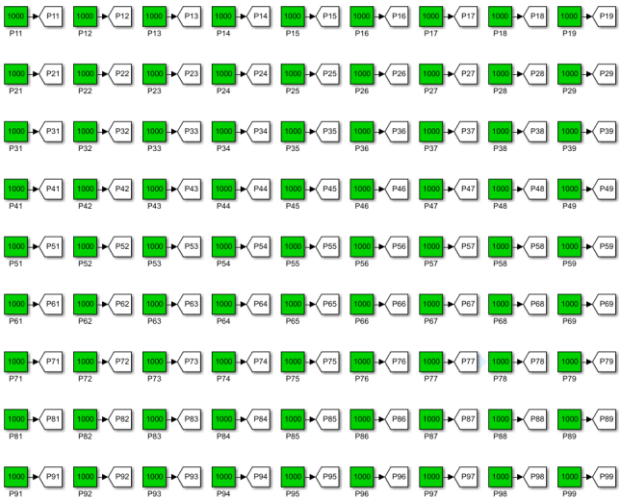

c) Irradiation Block

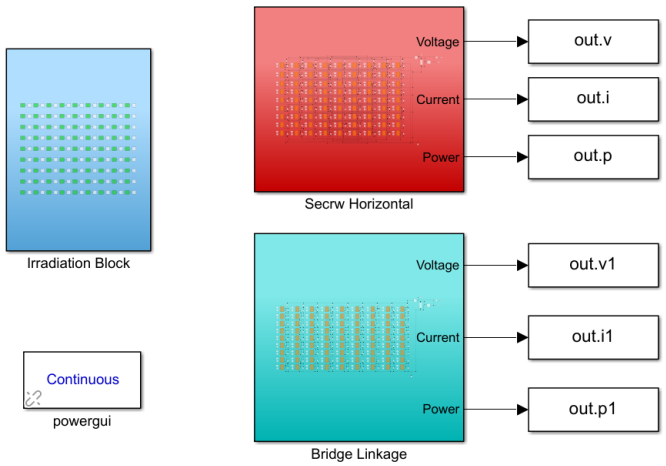

d) Simulation System

Figure 3. Simulation Through MATLAB/Simulink

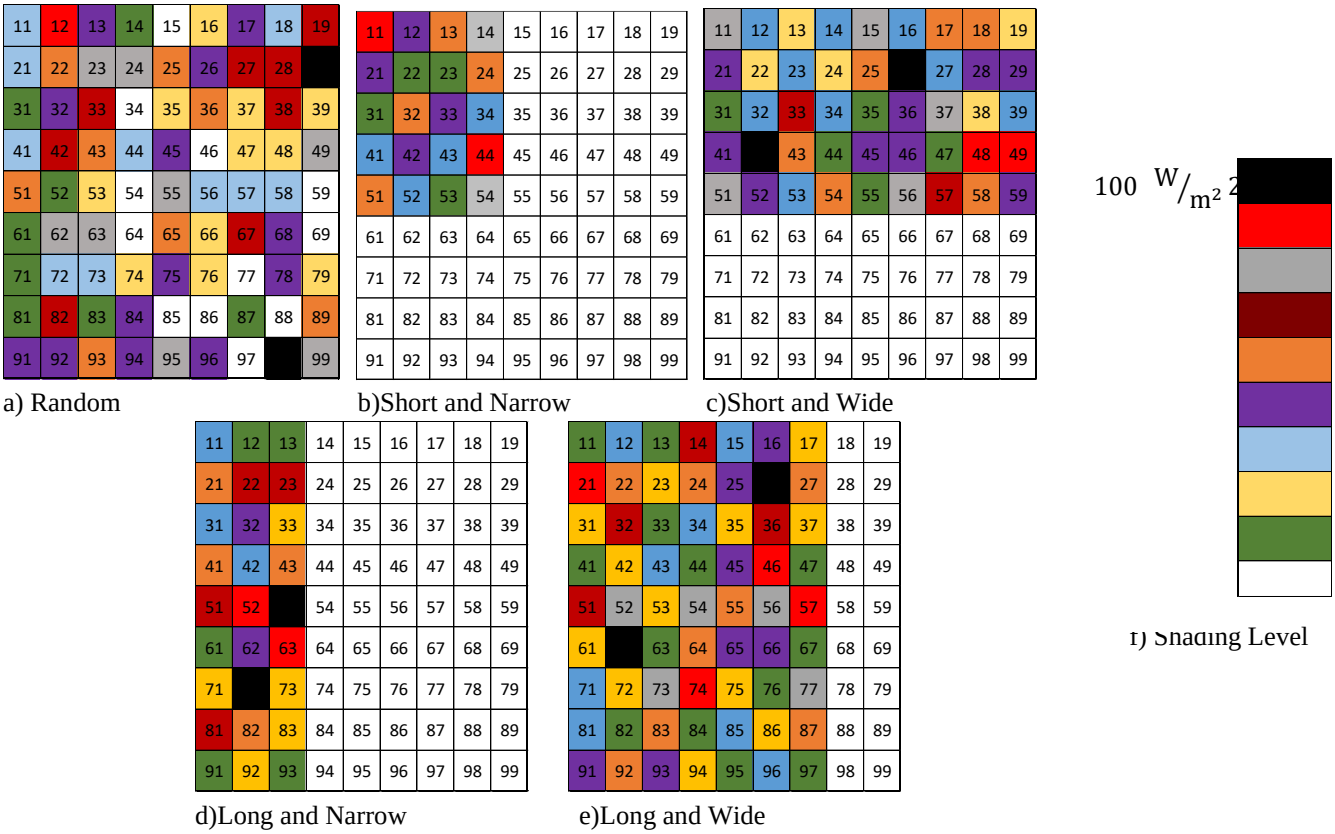

Figure 4. Proposed Shading

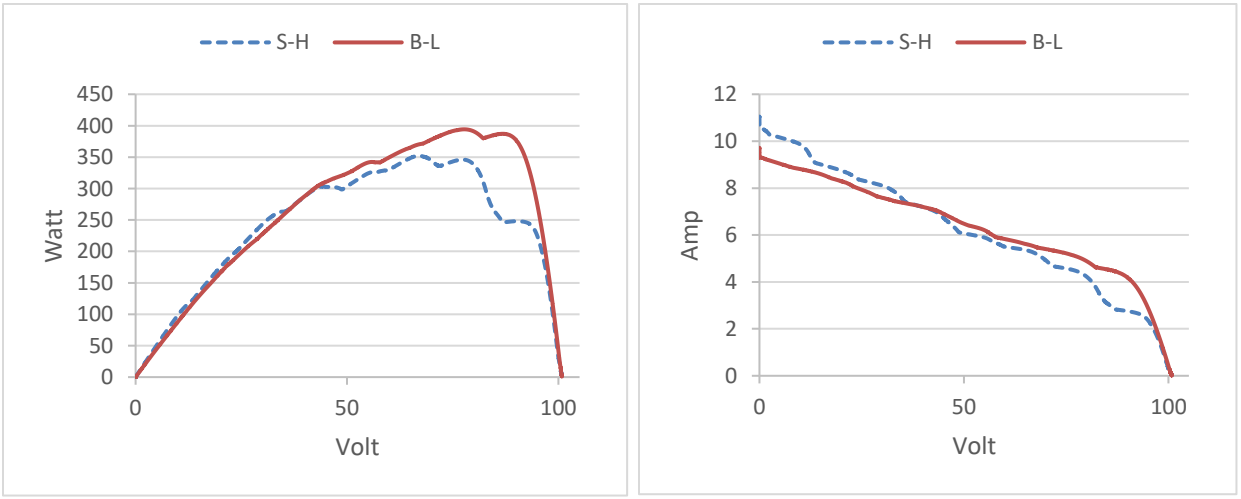

Figure 5. Random shading characteristics (P-V and I-V curves)

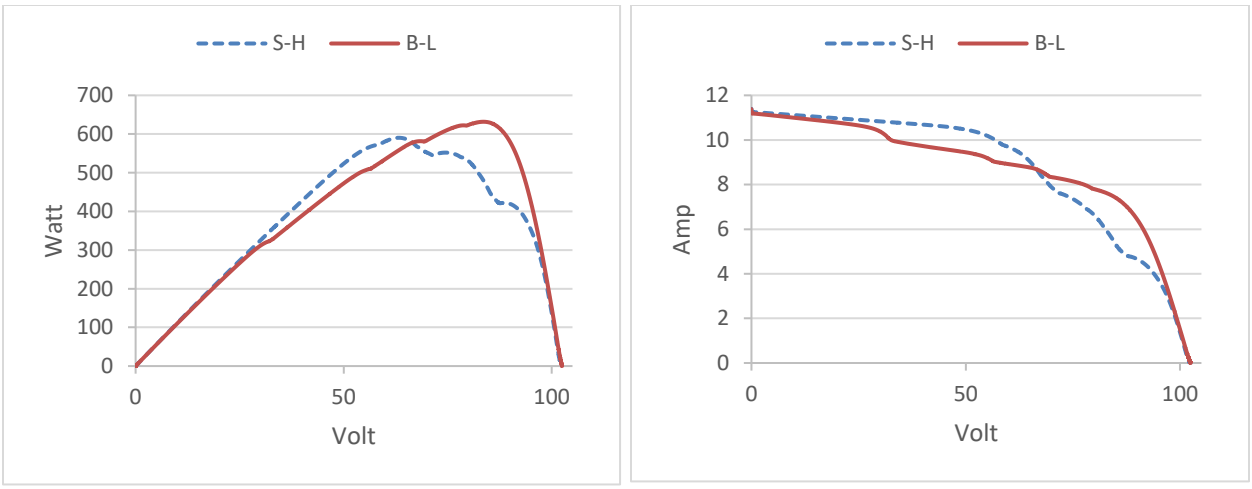

Figure 6. S&N shading characteristics (P-V and I-V curves)

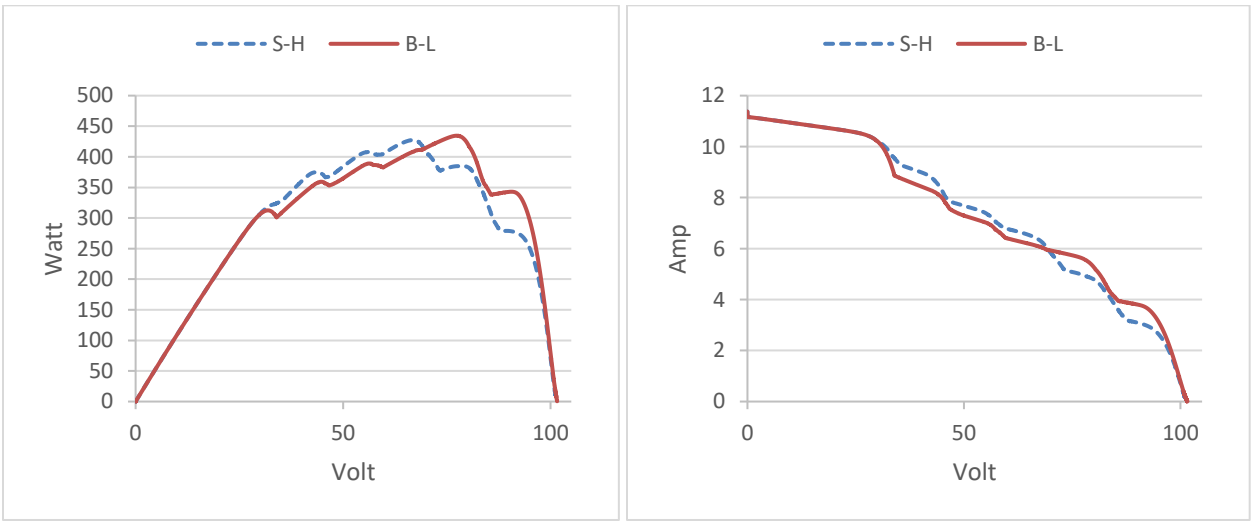

Figure 7. S&W shading characteristics (P-V and I-V curves)

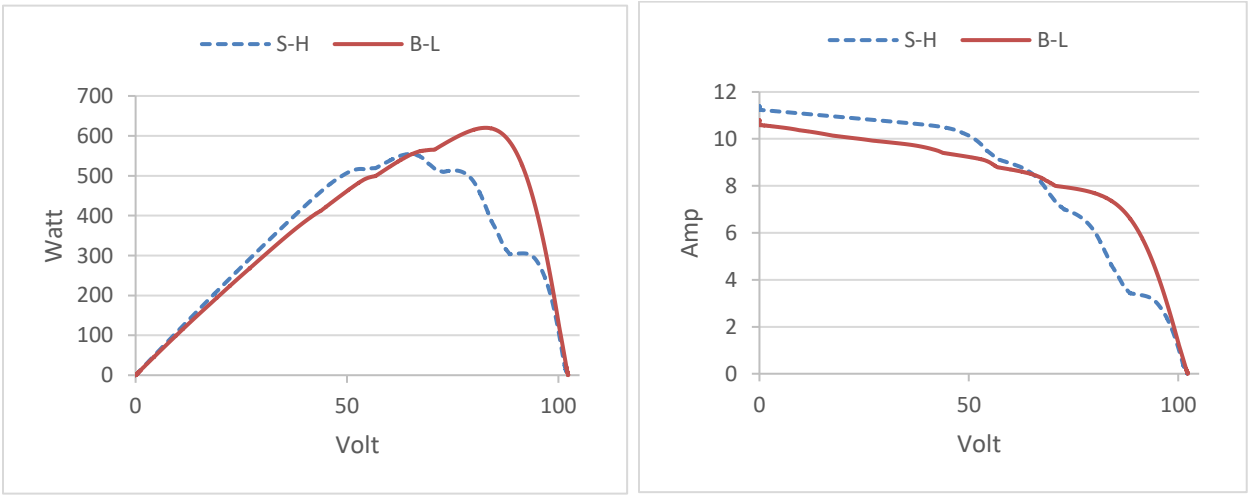

Figure 8. L&N shading characteristics (P-V and I-V curves)

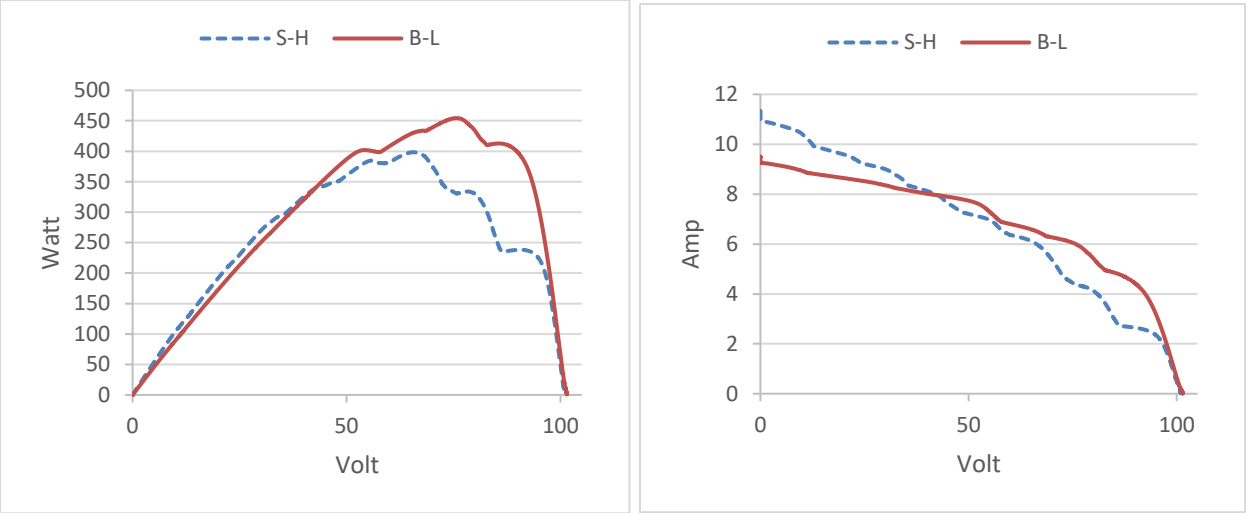

Figure 9. L&W shading characteristics (P-V and I-V curves)

According to the above characteristic curves, we can obtain the solar system's maximum power point and its voltage and current at that point. However, based on these values, we can apply Equations (1) to (5) to measure the performance analysis parameters that are shown in Table 1. Furthermore, the highest values of maximum power, voltage at maximum power, current at maximum power, fill factor, and efficiency indicate the system has the most efficient performance, otherwise, the lowest values of mismatch losses, power losses, and number of local maximum power peaks show that the system has the most optimal performance as well. Fig. 10 shows a comparison of the system's performance during five shading conditions.

Table 1. Simulation results and performance analysis

Configurations	**Screw Horizontal (S-H)**					**Bridge Linkage (B-L)**				
Shading patterns	Random	S&N	S&W	L&N	L&W	Random	S&N	S&W	L&N	L&W
P_{max} (W)	352.1	590.22	427.47	554.86	398.34	394.2	631.63	434.51	620.12	454.38
V_{mp} (V)	67.04	63.29	66.90	65.13	65.65	77.72	83.61	77.38	82.74	75.708
I_{mp} (A)	5.25	9.325	6.3889	8.518	6.06	5.071	7.55	5.614	7.49	6.001
FF (%)	30.07	50.41	36.51	47.39	34.023	33.67	53.95	37.11	52.96	38.810
ML (W)	449.55	211.44	374.20	246.81	403.33	407.45	170.03	367.16	181.55	347.29
PL (%)	56.07	26.37	46.67	30.78	50.31	50.82	21.21	45.79	22.64	43.321
ɳ (%)	43.92	73.62	53.32	69.21	49.68	49.17	78.78	54.20	77.35	56.67
LMPP's	3	2	4	3	3	2	1	4	1	2

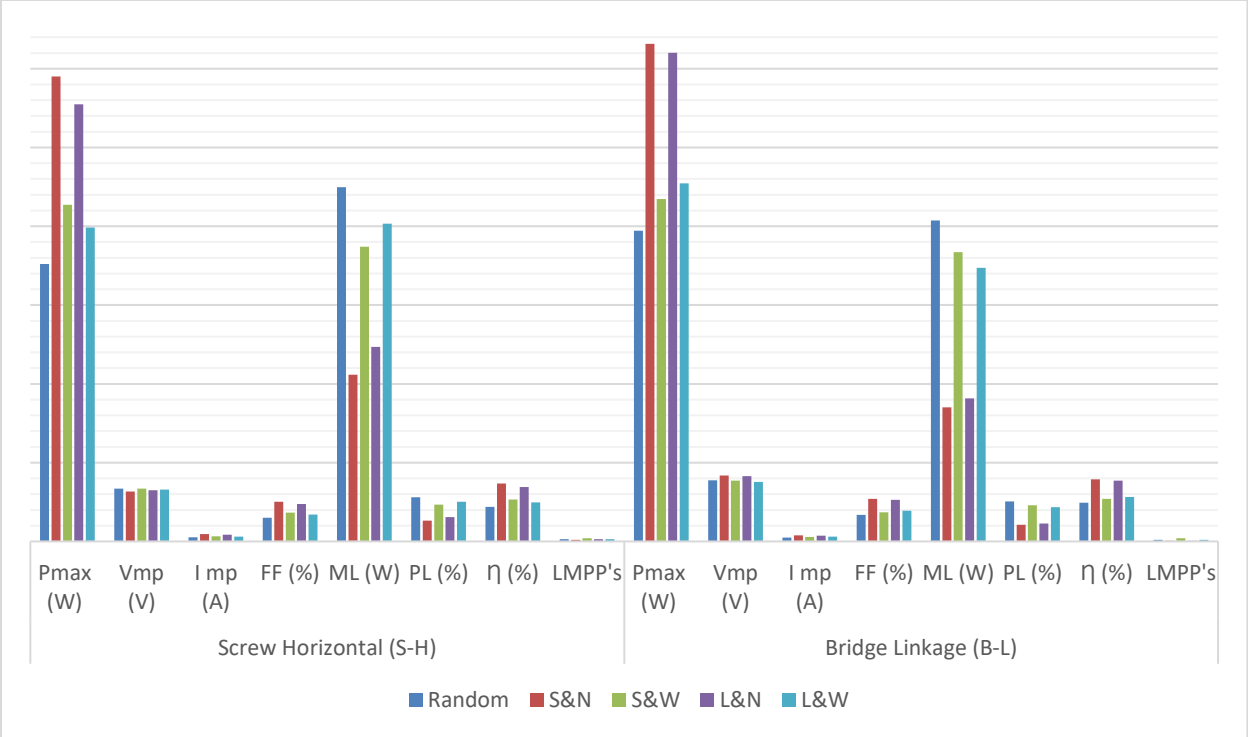

Figure 10. Performance comparison of proposed solar systems

6. Conclusion

According to the simulation results, the Bridge Linkage PV array configuration performs better than the Screw Horizontal array under partial shading conditions (PSCs). However, by comparing these photovoltaic array configurations, the maximum output power (P_{max}) of the (B-L) array is superior by 42.1W, 41.41W, 7.04W, 65.26W, and 56.04W respectively, furthermore, it produces higher percentage fill factor (FF) of 3.6%, 3.54%, 0.6%, 5.57%, and 4.787% respectively, compared to the (S-H) array. A Bridge Linkage array is more efficient than a Screw Horizontal array in the sense that (S-H) configuration has higher power losses by 5.25%, 5.16%, 0.88%, 8.14% and 6.99%, respectively, as a result (S-H) array has higher mismatch losses by 42.1W, 41.41W, 7.04W, 65.26W, and 56.04W respectively, as compared with (B-L) array. Additionally, the number of (LMPPs) represents one of the critical elements in determining the performance of PV systems, although most researchers do not give it any importance in their studies; therefore, the smoothest P-V curve (least number of LMPPs) indicates the most suitable configuration; however, the (B-L) array has a fewer number of LMPPs according to all shading conditions except (S&N) shading, where both configurations are equal. As for voltage and current at the maximum power point, the (B-L) array has higher voltage productivity by 10.68V, 20.32V, 10.48V, 17.61V, and 10.058V respectively, but the (S-H) array has better current productivity by 0.179A, 1.775A, 0.7749A, 1.028A and 0.059A respectively, than the (B-L).

When comparing the proposed configurations with [39] It can be observed. The authors in [39] do not examine all performance parameters that indicate which PV system is better, but they

focus on efficiency and maximum output power only. To determine which PV array would be better, we considered all performance parameters, including maximum output power, fill factor, mismatch losses, power losses, efficiency, and number of local maximum power peaks, as well as voltage and current at global maximum power peaks. Moreover, the authors in [39] use only the Static Reconfiguration Technique, while the proposed study combines the Static Reconfiguration Technique and Diodes Technique (Blocking and bypassing diodes). Although these diodes have a small voltage drop when they are operating under forward bias, bypass diodes offer excellent protection against fires caused by partial shading, and blocking diodes provide excellent protection against reverse currents from a discharging battery during the night. As a result, our study can be implemented practically and safely as compared with the study in [39] which cannot be implemented in practice. Lastly, our study compares two modern configurations (S-H) and (B-L), while [39] compares screw structure propagation arrays with old configurations such as (P-S), (TCT), and Sudoku configurations.

Future Work

1. Implemented our PV system practically.
2. Modify the type of bypass diodes and blocking diodes to another type to minimize the forward bias voltage drop.
3. Taking into account cable losses.
4. Measure the estimated life of each configuration.
5. A modern algorithm is used to overcome the multiple peaks in the PV system's output characteristics curve.
6. PV system behavior during loads should be checked.

Acknowledgments

This scientific paper is part of a master's thesis in the Electrical Engineering Department, College of Engineering, Mustansiriyah University. As well, the authors would like to thank each person at the university who assisted in completing this scientific paper.

Abbreviations

ML	Mismatch Losses
PL	Power Losses
η	Efficiency
FF	Fill Factor
STC	Standard Test Condition
PSC	Partial Shading Condition
P_m	Maximum Output Power
V_{mp}	Voltage at Maximum Power
I_{mp}	Current at Maximum Power
$V_{o.c}$	Voltage at open circuit condition
$I_{s.c}$	Current at short circuit condition
GMPP	Global maximum power peak
LMPP	Local maximum power peak
P-S	Parallel-Series configuration
TCT	Total Cross-tied configuration
S-V	Screw Vertical configuration
S-H	Screw Horizontal configuration
A-CT	Adaptive cross-tied configuration
FA	Firefly algorithm
B-L	Bridge Linkage configuration
CSP	Concentrated solar power
H-C	Honey combo configuration

Conflict of interest

The authors declare that there are no conflicts of interest regarding the publication of this paper.

Author Contribution Statement

The authors confirm their contribution to the paper as follows:

Author Mohammed Osamah Subhi: contributed to writing, analysis, discussion, and interpretation of the results of this manuscript.

Author Wafaa Saeed Majeed: proposed the research problem and supervised the findings.

Both authors reviewed the results and approved the final version of the manuscript.

References

1. C, Krauss The New York Times, (2014). *An oil industry awash in crude argues over exporting"*, [Online]. Available: https://www.nytimes.com/2014/02/13/business/energy-environment/an-oil-industry-awash-in-crude-argues-over-exporting.html
2. D. L. Greene, J. L. Hopson, and J. Li, (2006). *Have we run out of oil yet? Oil peaking analysis from an optimist's perspective*. Energy Policy. Vol. 34, no. 5, pp. 515–531. https://doi.org/10.1016/j.enpol.2005.11.025
3. H. A. Kazem, (2011). *Renewable energy in Oman: Status and future prospects*. Renewable and Sustainable Energy Reviews. Vol. 15, no. 8, pp. 3465–3469. https://doi.org/10.1016/j.rser.2011.05.015
4. A. A. Dehghan, (2011). *Status and potentials of renewable energies in Yazd Province-Iran*. Renew. Renewable and Sustainable Energy Reviews. Vol. 15, no. 3, pp. 1491–1496. https://doi.org/10.1016/j.rser.2010.11.002
5. Y. Anagreh, A. Bataineh, and M. Al-Odat, (2010). *Assessment of renewable energy potential, at Aqaba in Jordan*. Renewable *and* Sustainable Energy Reviews. Vol. 14, no. 4, pp. 1347–1351. https://doi.org/10.1016/j.rser.2009.12.007
6. M. T. Chaichan and H. A. Kazem, (2011). *Thermal storage comparison for variable basement kinds of a solar chimney prototype in Baghdad-Iraq weathers.* International Journal of Applied Science. Vol. 2, no. 2, pp. 12–20.
7. R. York and S. E. Bell, (2019). *Energy transitions or additions?: Why a transition from fossil fuels requires more than the growth of renewable energy* .Energy Research & Social Science. Vol. 51, pp. 40–43. https://doi.org/10.1016/j.erss.2019.01.008
8. M. Aminul Islam, Nabilah M. Kassim, Ammar A. A. and N. Amin, (2012). *Assessing the Impact of Spectral Irradiance on the Performance of Different Photovoltaic Technologies.* Intech open p.1-29. https://doi.org/10.5772/intechopen.96697
9. D. Y. Mahmood, A. H. Numan, and J. K. Ateih, (2019). *Simple and efficient control method for battery charging in high penetration photovoltaic array*. International Research Journal of Engineering and Technology. Vol. 6, no. 5, pp. 1813–1819.
10. D. Yousri, T. S. Babu, S. Mirjalili, N. Rajasekar, and M. Abd Elaziz, (2020). *A novel objective function with artificial ecosystem-based optimization for relieving the mismatching power loss of large-scale photovoltaic array*. Energy Conversion and Management. Vol. 225, pp. 113385.

11. https://doi.org/10.1016/j.enconman.2020.113385
12. Premkumar Manoharan, Umashankar Subramaniam, Thanikanti S. Babu, Sanjeevikumar Padmanaban, Jens B. Holm-Nielsen, Massimo Mitolo and Sowmya Ravichandran, (2020). *Improved perturb and observation maximum power point tracking technique for solar photovoltaic power generation systems*. IEEE Systems Journal. Vol. 15, no. 2, pp. 3024–3035.
13. https://doi.org/10.1109/jsyst.2020.3003255
14. W. C. Sinke, (2019). *Development of photovoltaic technologies for global impact*. Renewable Energy. Vol. 138, pp. 911–914. https://doi.org/10.1016/j.renene.2019.02.030
15. X. Ju, C. Xu, Y. Hu, X. Han, G. Wei, and X. Du, (2017). *A review on the development of photovoltaic/concentrated solar power (PV-CSP) hybrid systems*. Solar Energy Mater. Sol. Cells. Vol. 161, pp. 305–327. https://doi.org/10.1016/j.solmat.2016.12.004
16. A. Touil, M. Laissaoui, D. Nehari, and Y. H. Madani, (2017). *Study and optimization of thermal parameters of parabolic trough power plant used in the site of Ain-Defla*. NAT Technology. No. 16, p. 44.
17. V. Kaartemo, (2016). *In Climate Change and the 2030 Corporate Agenda for Sustainable Development*. Vol. 19, Emerald Group Publishing Limited, pp. 227–247. https://doi.org/10.1108/s2051-503020160000019011
18. P. Viebahn, Y. Lechon, and F. Trieb, (2011). *The potential role of concentrated solar power (CSP) in Africa and Europe—A dynamic assessment of technology development, cost development and life cycle inventories until 2050.* Energy Policy, vol. 39, no. 8, pp. 4420–4430. https://doi.org/10.1016/j.enpol.2010.09.026
19. M. A. Al Mamun, M. Hasanuzzaman, and J. Selvaraj, (2017). *Experimental investigation of the effect of partial shading on photovoltaic performance*. IET Renewable Power Generation. Vol. 11, no. 7, pp. 912–921. https://doi.org/10.1049/iet-rpg.2016.0902
20. A. H. Hameed and Y. S. Aljorany, (2011). *Investigation on nutrient behavior along Shatt Al-Arab River, Basrah, Iraq*. Journal of Applied Sciences Research. Vol. 7, no. 8, pp. 1340–1345.
21. P. Manganiello, M. Balato, and M. Vitelli, (2015). *A survey on mismatching and aging of PV modules: The closed loop*. IEEE Transactions on Industrial Electronics. Vol. 62, no. 11, pp. 7276–7286.
22. https://doi.org/10.1109/tie.2015.2418731
23. G. S. Krishna and T. Moger, (2019). *Reconfiguration strategies for reducing partial shading effects in photovoltaic arrays: State of the art*. Solar Energy. Vol. 182, pp. 429–452. https://doi.org/10.1016/j.solener.2019.02.057
24. P. O. Singh, (2011). *Modeling of photovoltaic arrays under shading patterns with reconfigurable switching and bypass diodes*. Thesis, Electrical Engineering Department, University of Toledo. https://etd.ohiolink.edu/acprod/odb_etd/ws/

send_file/send?accession=toledo1321559036&disposition=inline

25. P. K. Bonthagorla and S. Mikkili, (2020). *Performance analysis of PV array configurations (SP, BL, HC and TT) to enhance maximum power under non-uniform shading conditions*. Engineering Reports. Vol. 2, no. 8, p. e12214. https://doi.org/10.1002/eng2.12214
26. K. A. K. Niazi, Y. Yang, and D. Sera, (2019). *Review of mismatch mitigation techniques for PV modules*. IET Renewable Power Generation. Vol. 13, no. 12, pp. 2035–2050.
27. https://doi.org/10.1049/iet-rpg.2019.0153
28. J. C. Teo, R. H. G. Tan, V. H. Mok, V. K. Ramachandaramurthy, and C. Tan, (2020). *Impact of bypass diode forward voltage on maximum power of a photovoltaic system under partial shading conditions.* Energy. Vol. 191, p. 116491. https://doi.org/10.1016/j.energy.2019.116491
29. S. Anjum, V. Mukherjee, and G. Mehta, (2021). *Performance enhancement of photovoltaic array configurations with blocking p-MOSFETs under partial shading condition*. Energy Sources, Part A: Recovery, Utilization, and Environmental Effects. Vol. 43, no. 20, pp. 2509–2528. https://doi.org/10.1080/15567036.2020.1849455
30. P. R. Satpathy and R. Sharma, (2020). *Parametric indicators for partial shading and fault prediction in photovoltaic arrays with various interconnection topologies.* Energy Conversion and Management. vol. 219, p. 113018. https://doi.org/10.1016/j.enconman.2020.113018
31. P. Guerriero, P. Tricoli, and S. Daliento, (2019). *A bypass circuit for avoiding the hot spot in PV modules*. Solar Energy. Vol. 181, pp. 430–438. https://doi.org/10.1016/j.solener.2019.02.010
32. K. Lappalainen and S. Valkealahti, (2020). *Number of maximum power points in photovoltaic arrays during partial shading events by clouds*. Renewable Energy. Vol. 152, pp. 812–822.
33. https://doi.org/10.1016/j.renene.2020.01.119
34. A. Mäki and S. Valkealahti, (2013). *Effect of photovoltaic generator components on the number of MPPs under partial shading conditions*. IEEE Transactions on Energy Conversion. Vol. 28, no. 4, pp.1008–1017. https://doi.org/10.1109/tec.2013.2274280
35. B. Veerasamy, T. Takeshita, A. Jote, and T. Mekonnen (2018). Mismatch loss analysis of PV array configurations under partial shading conditions. In 2018 7th International Conference on Renewable Energy Research and Applications, ICRERA, pp. 1162–1183. https://doi.org/10.1109/icrera.2018.8566949
36. D. P. Winston, S. Kumaravel, B. P. Kumar, and S. Devakirubakaran, (2020). *Performance improvement of solar PV array topologies during various partial shading conditions*. Solar Energy. Vol. 196, pp. 228–242. https://doi.org/10.1016/j.solener.2019.12.007

37. K.-H. Chao, P.-L. Lai, and B.-J. Liao, (2015). *The optimal configuration of photovoltaic module arrays based on adaptive switching controls*. Energy Conversion and Management. Vol. 100, pp. 157–167.

38. https://doi.org/10.1016/j.enconman.2015.04.080

39. T. Ramesh, K. Rajani, and A. K. Panda, (2020). *A novel triple-tied-cross-linked PV array configuration with reduced number of cross-ties to extract maximum power under partial shading conditions*. CSEE Journal of Power and Energy Systems. Vol. 7, no. 3, pp. 567–581. https://doi.org/10.17775/cseejpes.2020.00750

40. S. C. Christabel, A. Srinivasan, and D. P. Winston, (2016). *Couple matching best generation algorithm for partially shaded photovoltaic systems*. Journal of Electrical Engineering. Vol. 16, no. 3, pp. 382–391.

41. A. Srinivasan, S. Devakirubakaran, and B. M. Sundaram, (2020) . *Mitigation of mismatch losses in solar PV system–Two-step reconfiguration approach.* Solar Energy. Vol. 206, pp. 640–654.

42. https://doi.org/10.1016/j.solener.2020.06.004

43. S. Kuram, P. Kuram, K. Raj, M. Kiran, D. Butti, S. Devakiru., T. Sudhakar, and H. Haes, (2021). *Power enhancement in partial shaded photovoltaic system using spiral pattern array configuration scheme*. IEEE Access. Vol. 9, pp. 123103–123116,

44. https://doi.org/10.1109/access.2021.3109248

45. M. N. R. Nazeri, M. F. N. Tajuddin, T. Sudhakar Babu, A. Azmi, M. Malvoni, and N. Manoj Kumar, (2021). *Firefly algorithm-based photovoltaic array reconfiguration for maximum power extraction during mismatch conditions*. Sustainability (Switzerland). Vol. 13, no. 6. https://doi.org/10.3390/su13063206

46. R. K. Pachauri, H. H. Alhelou, J. Bai, and M. E. H. Golshan, (2021). *Adaptive Switch Matrix for PV Module Connections to Avoid Permanent Cross-Tied Link in PV Array System under Non-Uniform Irradiations*. IEEE Access. Vol. 9. pp. 45978–45992. https://doi.org/10.1109/access.2021.3068637

47. N. Karuppiah, R. Muniraj, S. Kuram B., P. Kumar, T. Sudhakar, K. Raj, and H. Haes, (2021). *Performance Enhancement of Partial Shaded Photovoltaic System With the Novel Screw Pattern Array Configuration Scheme* .IEEE Access. Vol. 10, pp. 1731–1744. https://doi.org/10.1109/access.2021.3138917

48. S. R. Pendem and S. Mikkili, (2018). *Modelling and performance assessment of PV array topologies under partial shading conditions to mitigate the mismatching power losses*. Solar Energy. Vol. 160, pp. 303–321. https://doi.org/10.1016/j.solener.2017.12.010

49. M. Alanazi, A. Fathy, D. Yousri, and H. Rezk, (2022). *Optimal reconfiguration of shaded PV based system using African vultures optimization approach*. Alexandria Engineering Journal. Vol. 61, no. 12, pp.

12159–12185. https://doi.org/10.1016/j.aej.2022.06.009

50. M. Palpandian, D. P. Winston, B. P. Kumar, C. S. Kumar, T. S. Babu, and H. H. Alhelou (2021). *A new ken-ken puzzle pattern based reconfiguration technique for maximum power extraction in partial shaded solar PV array*. IEEE Access. Vol. 9, pp. 65824–65837. https://doi.org/10.1109/access.2021.3076608

51. A. Srinivasan, S. Devakirubakaran, B. Meenakshi, Praveen K., Santhan K., D. Prince, T. Sudhakar B. and Hassan H. Alhelou. (2021). *L-Shape Propagated Array Configuration with Dynamic Reconfiguration Algorithm for Enhancing Energy Conversion Rate of Partial Shaded Photovoltaic Systems*. IEEE Access. Vol. 9. pp. 97661–97674. https://doi.org/10.1109/access.2021.3094736

52. H. Bellia, R. Youcef, and M. Fatima, (2014). *A detailed modeling of photovoltaic module using MATLAB*. NRIAG Journal of Astronomy and Geophysics. Vol. 3, no. 1, pp.53–61. https://doi.org/10.1016/j.nrjag.2014.04.001

53. A. Kumar, N. Gupta, and V. Gupta. (2017). *A comprehensive review on grid-tied solar photovoltaic system*. Journal of Green Engineering. Vol. 7, no. 1, pp. 213–254. https://doi.org/10.13052/jge1904-4720.71210